N75 11189

Experimental Studies on Thermodynamic Effects of Developed Cavitation

ROBERT S. RUGGERI

NASA Lewis Research Center

A method for predicting thermodynamic effects of cavitation (changes in cavity pressure relative to stream vapor pressure) is presented. The prediction method accounts for changes in liquid, liquid temperature, flow velocity, and body scale. Both theoretical and experimental studies used in formulating the method are discussed. The prediction method provided good agreement between predicted and experimental results for geometrically scaled venturis handling four different liquids of widely diverse physical properties. Use of the method requires geometric similarity of the body and cavitated region and a known reference cavity-pressure depression at one operating condition.

Because cavitation is a vaporization process that involves heat and mass transfer, the physical properties of the liquid and its vapor and the flow conditions can affect the cavitation process and thus the cavitation performance of hydraulic equipment as well. These combined effects of fluid properties, flow conditions, and heat transfer—termed thermodynamic effects of cavitation—can improve cavitation performance. For example, cavitation studies with pumps and pump inducers (refs. 1 through 6) have shown that, for certain liquids and/or liquid temperature, the net positive suction head (NPSH) requirements can be significantly less than those for room-temperature water. This improvement in inlet pressure requirements is attributed to the varying degrees of evaporative cooling associated with the cavitation process. Because of cooling, the vapor pressure of the liquid adjacent to the cavity and the cavity pressure itself are decreased relative to the vapor pressure of the bulk liquid. This decrease in cavity pressure retards the rate of further vapor formation, thereby allowing lower inlet pressures than are otherwise possible. For a given cavity size at fixed flow conditions, a reduction in cavity pressure allows a corresponding reduction in the inlet pressure requirements. The accurate prediction of the thermodynamic effects of

cavitation is therefore essential to an optimum system designed to operate with cavitation.

The objective of this paper is to summarize the results obtained from theoretical and supporting experimental venturi cavitation studies (refs. 7 through 11) which led to the formulation of a method for predicting thermodynamic effects of cavitation. The method was motivated by, but is an extension of, the *B*-factor concept of Stahl and Stepanoff (ref. 12). The prediction method accounts for changes in liquid, temperature, flow velocity, and scale. The cavitation data were obtained for Freon-114, liquid hydrogen, liquid nitrogen, and water using two accurately scaled venturis (1.0 and 0.7 scale) as test devices. The liquid hydrogen data were obtained from a NASA-sponsored study conducted at the National Bureau of Standards (ref. 11). The data for the other liquids (refs. 7 through 10) were obtained at the NASA Lewis Research Center.

ANALYTICAL REVIEW

Thermodynamic Effects of Cavitation

Heat is required to generate the vapor within a cavitated region, and this heat of vaporization must be drawn from the surrounding liquid. If the time available for vaporization is short, as is usually the case for flowing systems, the liquid which supplies the heat for vaporization consists of a relatively thin film of liquid adjacent to the cavity. Cooling of this film causes the vapor pressure of both the liquid film and the vaporous cavity to drop from that of the bulk liquid to that corresponding to the reduced local temperature. For a cavity of given size with fixed flow conditions, a reduction in cavity pressure allows a corresponding reduction in the inlet pressure requirements. Thus the inlet pressure requirement for a particular flow device handling liquids which exhibit significant drops in cavity pressure is less than that for liquids which do not exhibit this beneficial effect. In general, cavity-pressure and temperature depressions (thermodynamic effects of cavitation) are a function of fluid properties as well as the body geometry, the flow velocity, and the complex heat and mass transfer mechanisms involved.

Heat Balance

The magnitude of cavity-pressure depression can be estimated by setting up (as an initial step) a heat balance between the heat required for vaporization and the heat drawn from the liquid surrounding the cavity; that is,

$$\rho_v v_v L = \rho_l v_l c_l (\Delta T) \tag{1}$$

where v_l represents the volume of the thin layer of liquid that is cooled

during vaporization. Although applied to cavitation in a flowing system herein, the energy balance (eq. (1)) is equivalent to a static model of a simple insulated cylinder-piston model (ref. 13). A given mass of liquid fills the cylinder. With an increase in total volume, achieved by lifting the piston, some of the liquid is vaporized. The heat required to form the vapor that fills the resulting increased volume must be drawn from the remaining liquid, thereby lowering the temperature by some amount ΔT. The primary assumptions associated with the heat balance (eq. (1)) are discussed in reference 8.

By expressing the temperature drop ΔT (eq. (1)) in terms of a vapor-pressure drop Δh_v, through use of the vapor-pressure temperature relations, equation (1) may be expressed in the form

$$\Delta h_v = \frac{\rho_v}{\rho_l} \frac{v_v}{v_l} \frac{L}{c_l} \left(\frac{dh_v}{dT}\right) \tag{2}$$

where dh_v/dT is the slope of the vapor-pressure/temperature curve at the temperature of interest. All the terms in equation (2) are fluid properties and are known except the vapor- to liquid-volume ratio v_v/v_l. In the experimental case the absolute value of volume ratio cannot be directly determined because v_l is only that volume of liquid actually involved in the vaporization process. Thus v_l is only a fraction of the entire liquid stream. However, as shown in equation (2), the parameter Δh_v can be expressed as a function of v_v/v_l for any liquid whose fluid properties are known. To account for changes in fluid properties as the temperature decreases due to vaporization, equation (2) may be solved (in terms of Δh_v versus v_v/v_l) in incremental form. That is, suitably small increments of Δh_v are assumed, and the results from successive steps are summed to yield v_v/v_l. Results obtained in this manner for water, liquid nitrogen, Freon-114, and liquid hydrogen at various initial fluid temperatures are presented in figure 1. The nonlinearity of the curves is due to the change in fluid properties as the equilibrium temperature drops due to vaporization.

For a given value of v_v/v_l, the depression in cavity pressure can vary by several orders of magnitude depending on liquid and liquid temperature.

By using the Clasius-Clapeyron equation to approximate the slope of the vapor-pressure/temperature curve, the following useful approximation of equation (2)—and thus the curves of figure 1—is obtained:

$$\Delta h_v \cong J \left(\frac{\rho_v}{\rho_l}\right)^2 \left(\frac{L^2}{c_l T}\right) \left(\frac{v_v}{v_l}\right) \tag{3}$$

This expression provides a useful and close approximation of the curves presented in figure 1.

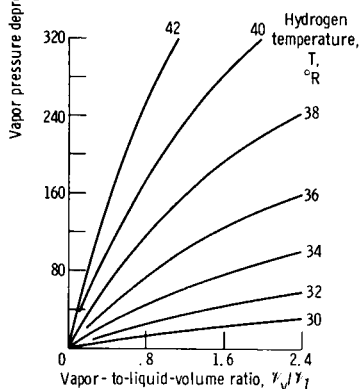a.—*Water, liquid nitrogen, and Freon-114.*
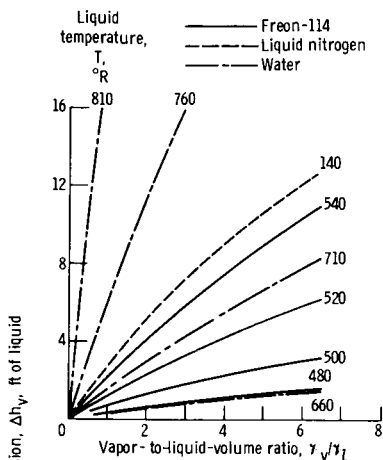
b.—*Liquid hydrogen.*

FIGURE 1.—*Vapor pressure depressions for various liquids and liquid temperatures.*

As previously discussed, the vapor-to-liquid-volume ratio ν_v/ν_l in any real flow situation is not known and cannot be measured directly. Thus values of the ν_v/ν_l ratio from figure 1 are used only in a relative sense. However, useful predictions for geometrically similar cavities may be made as follows. By experiment, an effective or reference value of ν_v/ν_l is established through the determination of cavity-pressure depressions Δh_v for one flow devic̣e, liquid, temperature, and velocity. Then values of ν_v/ν_l for other geometrically similar flow devices, liquids, liquid temperatures, and flow velocities may be estimated relative to this reference value, as described subsequently. With these predicted values of ν_v/ν_l and figure 1, determination of Δh_v relative to reference data is possible.

Estimation of Vapor-to-Liquid Volume Ratio

In the overall systematic study of thermodynamic effects of cavitation, several theoretical analyses for estimating vapor-to-liquid-volume ratio

were made. However, in the interest of brevity, only the pertinent relations and a short discussion of these analyses is presented. Details of the various derivations are presented in the references cited.

The theoretical analysis of reference 8 shows that for one body scale, the vapor-to-liquid-volume ratio v_v/v_l can be predicted for changes in the liquid used, the temperature, the velocity, and the cavity length, provided that a reference value of v_v/v_l is known. Subsequently this study was extended to include the effects of geometric scaling (ref. 9). The combined results from references 8 and 9 led to the following general equation (see ref. 10) for predicting the vapor-to-liquid-volume ratio, relative to a reference value, for changes in liquid, liquid temperature, flow velocity, and model scale:

$$\left(\frac{v_v}{v_l}\right)_{\text{pred}} = \left(\frac{v_v}{v_l}\right)_{\text{ref}} \left(\frac{\alpha_{\text{ref}}}{\alpha}\right)^m \left(\frac{V_0}{V_{0,\text{ref}}}\right)^n \left(\frac{D}{D_{\text{ref}}}\right)^{1-n} \left[\frac{(\Delta x/D)_{\text{ref}}}{\Delta x/D}\right]^p \quad (4)$$

where α is thermal diffusivity, V_0 is free-stream velocity, D is diameter, and Δx is the axial length of the cavitated region. The exponents m, n, and p depend, at least in part, on the heat transfer process involved and must be determined by experiment. The derivation and use of equation (4) requires, first, that geometric similarity of cavitating flow is maintained for various liquids and flow conditions and, second, that thermodynamic equilibrium conditions exist within the cavitated region. At present, these two requirements can only be assumed for untested liquids.

EXPERIMENTAL VENTURI STUDIES

In order to determine the exponents for the theoretically derived equation (4), it was necessary to conduct cavitation studies in such a way that the temperatures and pressures within cavitated regions of various liquids could be measured directly. Accurately scaled venturis (1.0 and 0.7 scale) were used as test flow devices. In order to provide a wide range of physical properties, Freon-114, liquid hydrogen, liquid nitrogen, and water were used as test fluids. The fluids were studied over a range of approach flow velocities (100 to >200 ft/sec for liquid hydrogen and ~19-50 ft/sec for the other liquids).

Venturis

The venturis, made of transparent acrylic plastic, incorporated a circular arc contour to provide convergence from the approach section to a constant-diameter throat section (fig. 2). The throat section is followed by a conical diffuser. The venturi with the 1.743-inch approach-section diameter is referred to herein as the 1.0-scale venturi, and that

FIGURE 2.—*Venturi test sections (all dimensions in inches).*
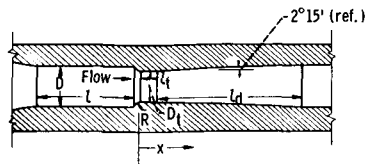
	Venturi scale	
	1.0	0.7
Free-stream diameter, D	1.743	1.232
Throat diameter, D_t	1.377	0.976
Radius of curvature, R	0.183	0.128
Approach-section length, l	4.198	2.964
Throat length, l_t	0.75	0.52
Diffuser length, l_d	4.66	3.26

with the 1.232-inch approach section diameter is referred to as the 0.7-scale venturi. Detailed descriptions of the venturis are given in references 7 through 9. The venturis were mounted either in a small, closed-return hydrodynamic tunnel of 10-gallon capacity (NASA facility, ref. 7) or in an NBS liquid hydrogen blowdown test facility (ref. 11) with the 0.7-scale venturi located between 265-gallon supply and receiver dewars.

The noncavitating wall-pressure distribution for the venturis is presented in figure 3. As stream pressure was lowered, cavitation occurred first at the point of minimum pressure located on the circular arc portion of the venturi. The cavity's leading edge was visually observed to remain fixed at the minimum pressure location for all cavitating conditions studied.
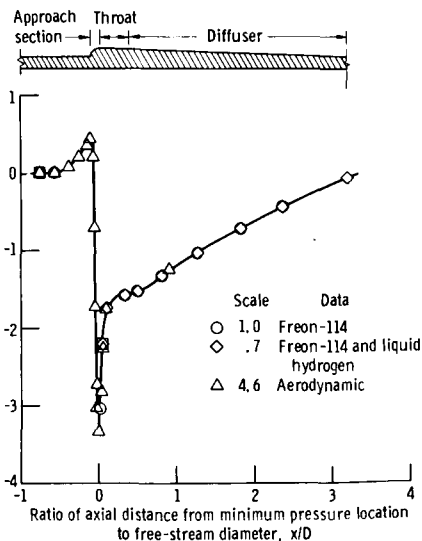

FIGURE 3.—*Wall pressure distribution for venturis.*

Appearance of Developed Cavitation

Photographs showing typical developed cavitation for Freon-114 and liquid hydrogen are presented in figure 4. Although the vapor formation in hydrogen was more homogeneous, the appearance of cavitation for these fluids was similar; that is, the cavities exhibit a uniform peripheral development with the leading edge at a fixed location. Because of this similarity in cavitating flow (a prerequisite in the analysis), the data obtained for both hydrogen and Freon-114 are considered equally valid for determining the exponents in the theoretical prediction equation. Temperatures and pressures within the relatively thin annulus of vapor formed (estimated thickness less than 0.03 inch in the throat) were measured simultaneously by pressure taps and calibrated thermocouples located on the adjacent wall.

RESULTS AND DISCUSSION

Specific trends in temperature and pressure depressions within cavitated regions of Freon-114 and liquid hydrogen are discussed first. Exponents in the theoretical prediction equation are then determined, and, finally, the significance of a developed cavitation similarity parameter $K_{c,min}$ is discussed.
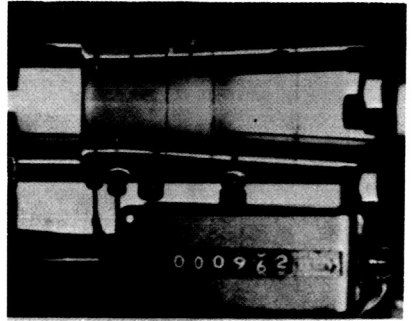
Typical Cavity Pressure and Temperature Distribution

A plot showing typical variations in pressure and temperature depressions within a constant-length cavity (Freon-114) is shown in figure 5. Cavity-pressure depression is presented as a function of x/D measured from the minimum pressure location determined with noncavitating flow. The data are for a cavity length of about 2.75 inches (comparable to that shown in fig. 4d) and a constant approach velocity of 31.8 feet per second. All pressures within the cavitated region are less than vapor pressure based on the free-stream temperature (represented by $\Delta h_v = 0$). The maximum measured cavity-pressure depression always occurred at or near the cavity's leading edge. The point at which the cavity pressure equals the vapor pressure of the bulk liquid ($\Delta h_v = 0$) coincides with the collapse region of cavitation. The open symbols represent cavity pressures measured directly, whereas the solid symbols represent the fluid vapor pressure corresponding to the locally measured temperature. The figures adjacent to the solid symbols represent measured reductions in local cavity temperature below the free-stream temperature. The good agreement between the measured pressures and the vapor pressures based on measured temperature indicate that, for engineering purposes, thermodynamic equibrilium conditions can be assumed to exist within the cavity.

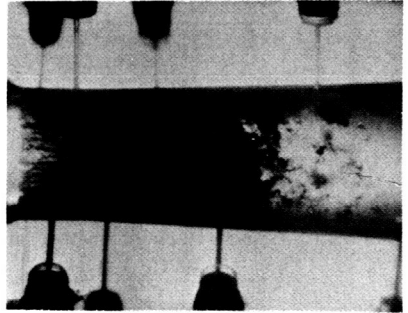a.—*Liquid hydrogen in 0.7-scale venturi; nominal cavity length, 1.0 freestream diameter.*
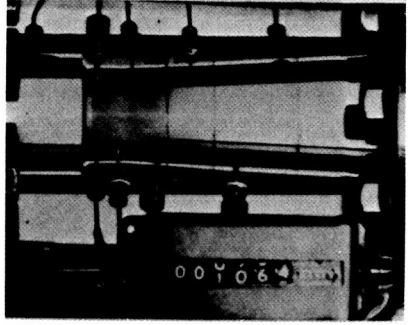
b.—*Liquid hydrogen in 0.7-scale venturi; nominal cavity length, 1.6 freestream diameters.*

c.—*Freon-114 in 0.7-scale venturi; nominal cavity length, 1.4 freestream diameters.*

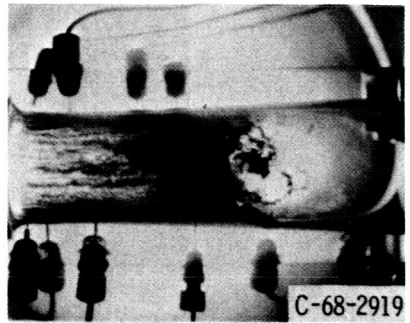d.—*Freon-114 in 1.0-scale venturi; nominal cavity length, 1.5 freestream diameters.*

FIGURE 4.—*Typical cavitation in venturis.*

Open symbols denote measured pressure
depression
Solid symbols denote vapor pressure
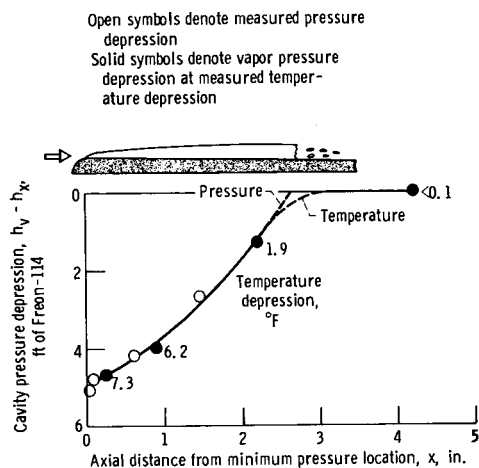depression at measured temper-
ature depression

FIGURE 5.—*Typical pressure and temperature depressions within cavitated region. Freon-114; 1.0-scale venturi; velocity, 31.8 feet per second; temperature, 519.1° R.*

Also, the studies showed that for fixed flow conditions and geometrically similar cavities, a change in the maximum cavity depression resulted in an equal change in the inlet pressure requirement (NPSH). This occurred for all liquids and temperatures studied.

Effects of Temperature, Flow Velocity, Cavity Length, and Scale

An increase in bulk liquid temperature caused an increase in cavity-pressure depression along the entire cavity length as illustrated in figure 6. For the conditions shown, the maximum cavity depression is about 8.5 feet of Freon-114 ($\sim$5.5 psi) at 538.8° R, which is about 1.7 times that at 519° R and 4.6 times that at 467.5° R. This trend with temperature was observed for all test liquids at each flow velocity studied. However, for water, over the 500° R to 580° R temperature range studied, the cavity-pressure drop was so small as to be negligible.

An increase in free-stream velocity caused an increase in cavity-pressure depressions. Some typical results are presented in figure 7. As velocity was increased from 22.9 to 44.5 feet per second, the maximum cavity depression increased from about 6.6 feet of Freon-114 to about 11.0 feet.

As cavity length was increased, the cavity-pressure depression increased over the full axial length of the cavity, as illustrated by the liquid hydrogen data (0.7-scale venturi) presented in figure 8. The trend shown is typical for the other liquids tested. For the conditions studied, the measured cavity-pressure depressions for hydrogen were about 50 to 100 times greater (in feet of liquid) than those for Freon-114. Maximum

FIGURE 6.—*Effect of free-stream liquid temperature on cavity pressure and temperature depressions. Freon-114, 1.0-scale venturi; nominal cavity length, 2.75-inches.*
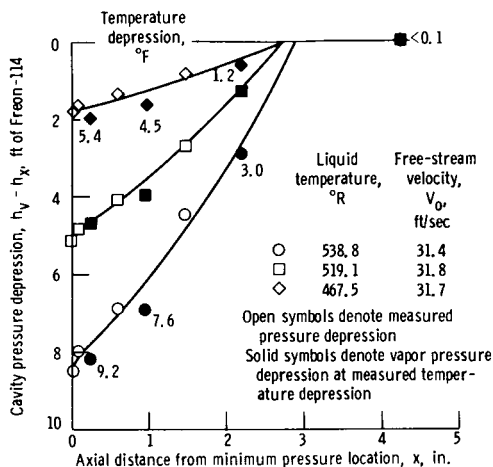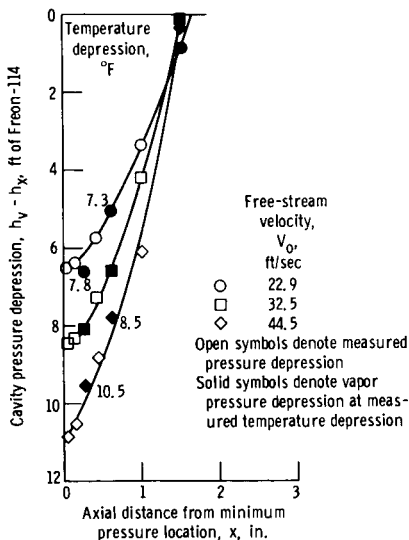
Liquid temperature, °R	Free-stream velocity, V_o, ft/sec
○ 538.8	31.4
□ 519.1	31.8
◇ 467.5	31.7

Open symbols denote measured pressure depression
Solid symbols denote vapor pressure depression at measured temperature depression

FIGURE 7.—*Effect of free-stream velocity on pressure and temperature depressions within cavitated regions of Freon-114. Venturi scale, 0.7; liquid temperature, 540° R; nominal cavity length, 1.6 inches.*

Free-stream velocity, V_o, ft/sec
○ 22.9
□ 32.5
◇ 44.5

Open symbols denote measured pressure depression
Solid symbols denote vapor pressure depression at measured temperature depression

depressions reached as much as 580 feet of hydrogen at the higher free-stream velocities and temperatures studied, compared to about 11 feet for Freon-114.

For geometrically similar cavities ($\Delta x/D = $ const), cavity-pressure depressions over the entire length of the cavity are little affected by model scale, at least for the modest range tested. This is illustrated in figure 9, where Freon-114 data obtained in both the 0.7- and 1.0-scale venturis are compared. Cavity-pressure depression is plotted as a function of the ratio of axial distance to free-stream diameter.
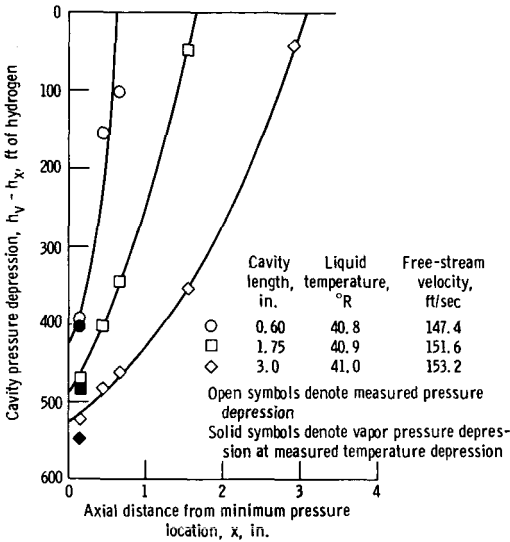
FIGURE 8.—*Effect of cavity length on cavity pressure depression. Liquid hydrogen; 0.7-scale venturi.*

Cavity length, in.	Liquid temperature, °R	Free-stream velocity, ft/sec
○ 0.60	40.8	147.4
□ 1.75	40.9	151.6
◇ 3.0	41.0	153.2

Open symbols denote measured pressure depression
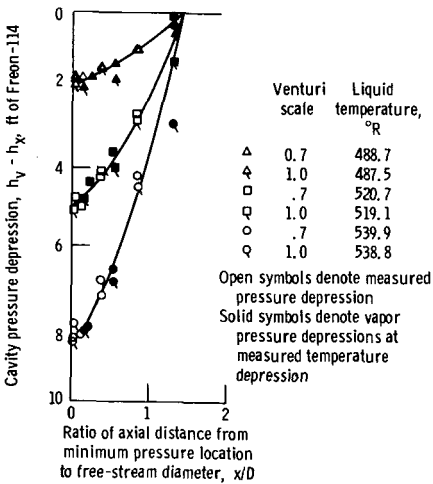Solid symbols denote vapor pressure depression at measured temperature depression

FIGURE 9.—*Effect of venturi scale on pressure and temperature depressions within cavitated regions of Freon-114. Cavity length, 1.4 free-stream diameters.*

	Venturi scale	Liquid temperature, °R
△	0.7	488.7
◮	1.0	487.5
□	.7	520.7
◖	1.0	519.1
○	.7	539.9
◗	1.0	538.8

Open symbols denote measured pressure depression
Solid symbols denote vapor pressure depressions at measured temperature depression

DETERMINATION OF EXPONENTS IN PREDICTION EQUATION

In all instances the maximum measured cavity-pressure depressions were used to determine the exponents for the equation for prediction of vapor-to-liquid-volume ratio ν_v/ν_l (eq. (4)). The Freon-114 data (for both the 1.0- and 0.7-scale venturis) and the hydrogen data (0.7-scale venturi) were used in conjunction with the method of least squares to

solve for all the exponents simultaneously. More than 100 data points were used. The resulting expression with the experimentally determined exponents is

$$\left(\frac{\nu_v}{\nu_l}\right)_{\text{pred}} = \left(\frac{\nu_v}{\nu_l}\right)_{\text{ref}} \left(\frac{\alpha_{\text{ref}}}{\alpha}\right)^{1.0} \left(\frac{V_0}{V_{0,\text{ref}}}\right)^{0.8} \left(\frac{D}{D_{\text{ref}}}\right)^{0.2} \left[\frac{\Delta x/D}{(\Delta x/D)_{\text{ref}}}\right]^{0.3} \quad (5)$$

The exponent for the diameter-ratio term presently comes via theory from the exponent n of the velocity-ratio term (see eq. (4)). Thus additional cavitation studies which use other scale factors are needed to further substantiate the exponent for D/D_{ref}.

From a measured value of Δh_v in a model of given scale, the volume ratio $(\nu_v/\nu_l)_{\text{ref}}$ can be determined from figure 1 (or eq. (2)). Equation (5) can then be used to determine $(\nu_v/\nu_l)_{\text{pred}}$ for the liquid, temperature, velocity, and scale of interest. With this value of $(\nu_v/\nu_l)_{\text{pred}}$, figure 1 can be used again to predict the corresponding value of Δh_v. For the present, equation (5), with the experimentally determined exponents, is offered as the best approach toward generalizing results for different scaled venturis, different liquids and liquid temperatures, and various velocities.

COMPARISON OF PREDICTED AND EXPERIMENTAL RESULTS

The agreement to be expected between experimental and predicted results is presented in figure 10. The complete test range of Δh_v values is presented in figure 10a, which emphasizes liquid-hydrogen data. The low range of values is presented in figure 10b. All points shown in figure 10 are based on a single reference point represented by the solid symbol. The reference value was obtained with 538° R Freon-114 in the 1.0-scale venturi at a free-stream velocity of 19.6 feet per second. The cavity length, $\Delta x/D$, was 0.72. The measured Δh_v was 5.0 feet of Freon-114, and thus the value of $(\nu_v/\nu_l)_{\text{ref}}$ (from fig. 1) was 2.6. Predicted values of ν_v/ν_l were then calculated from equation (5). All predicted Δh_v-values appear to be quite good, considering that predicted values of up to 600 feet of liquid (at $V_0 > 200$ ft/sec), were based on a single reference value of only 5.0 feet at 19.6 feet per second.

It is concluded that the simple static model analysis with experimentally determined exponents provides reasonably good predictions over a wide range of fluid properties and flow conditions, provided that (1) the maximum cavity-pressure depression is known for at least one operating condition, (2) similarity of cavitating flow is maintained, and (3) local equilibrium of temperature and pressure exists at the vapor/liquid interface.

Liquid	Venturi scale
○ Hydrogen	0.7
□ Freon-114	.7
▷ Nitrogen	1.0
◇ Freon-114	1.0
△ Water	1.0
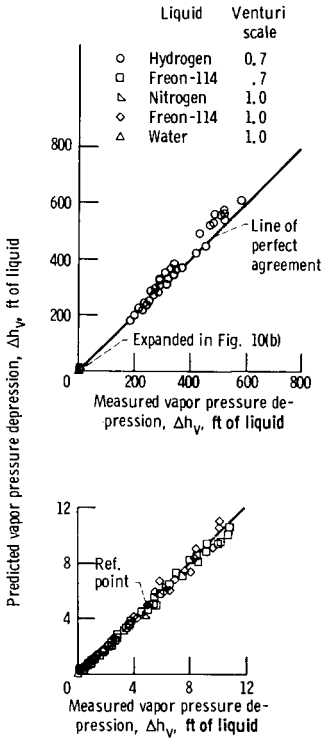
a.—*Complete range of vapor-pressure depressions.*

b.—*Low range of vapor-pressure depressions.*

FIGURE 10.—*Comparisons of measured and predicted vapor-pressure depressions.*

CAVITATION SIMILARITY PARAMETERS

The conventional cavitation parameter is usually expressed as

$$K_v \equiv \frac{h_0 - h_v}{V_0^2/2g} \tag{6}$$

The parameter K_v for developed cavitation is derived from the assumption that Bernoulli's equation for steady ideal flow applies between a free-stream location and the cavity surface and that the cavity surface is at a constant pressure equal to free-stream vapor pressure. However, because of the previously discussed thermodynamic effects of cavitation, the cavity pressure can be significantly less than free-stream vapor pressure and can also vary with axial distance. Thus, a more general expression for the cavitation parameter would have h_v in equation (6) replaced with a more appropriate reference pressure in the cavity. As in references 8 through 10, the maximum cavity-pressure depression is selected as the reference pressure to define the following developed cavitation parameter:

$$K_{c,min} = \frac{h_0 - h_{c,min}}{V_0^2/2g} = \frac{h_0 - h_v}{V_0^2/2g} + \frac{(\Delta h_v)_{max}}{V_0^2/2g} = K_v + \frac{(\Delta h_v)_{max}}{V_0^2/2g} \qquad (7)$$

The venturi cavitation studies show that $K_{c,min}$ is approximately constant over the range of liquids, temperatures, velocities, and venturi scales tested, provided that the geometric similarity of the cavitated region is maintained. The value of K_v however, varied widely.

The degree to which a constant value can be used to represent $K_{c,min}$ is shown graphically in figure 11, where the numerator of $K_{c,min}$ is plotted as a function of its denominator. The line shown is for a $K_{c,min}$ of 2.47. The good agreement between the data and the line indicates that a single $K_{c,min}$ value of 2.47 can be utilized to represent all the hydrogen and Freon-114 data. This $K_{c,min}$ value of 2.47 also applies quite well for liquid nitrogen and water. As previously stated, the cavity-pressure depressions for water were practically negligible; thus, the values of $K_{c,min}$ and the conventional cavitation parameter K_v were essentially the same for the range of water temperatures studied. Although the value of $K_{c,min}$ remained constant for different cavity lengths, it is possible that for other venturi shapes $K_{c,min}$ will vary with cavity length.

Prediction of Free-Stream Pressure Requirements

For constant values of $K_{c,min}$ and V_0 in equation (7), a change in $(\Delta h_v)_{max}$ results in a corresponding change in $h_0 - h_v$. This pressure

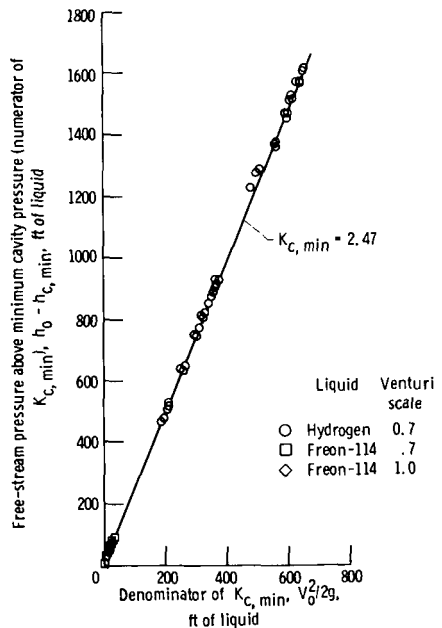

FIGURE 11.—Effects of venturi scale and liquid on minimum pressure of cavitated region. Various cavity lengths, $\Delta x/D$.

difference $h_0 - h_v$ is a measure of free-stream pressure requirements to obtain geometrically similar cavities and includes the thermodynamic effects of cavitation. Thus, for the wide range of conditions for which $K_{c,\text{min}}$ is constant, it is a most useful cavitation similarity parameter. When at least one value of $(\Delta h_v)_{\text{max}}$ (or $h_{c,\text{min}}$) is known and used as the reference value for predicting other values of $(\Delta h_v)_{\text{max}}$, as previously discussed, the free-stream pressure requirements h_0 for untested conditions can be predicted by equation (7). This equation can be rearranged so that

$$h_0 = \frac{V_0^2}{2g} (K_{c,\text{min}}) + h_v - (h_v - h_{c,\text{min}}) \qquad (8)$$

where $h_v - h_{c,\text{min}} = \Delta h_{v_{\text{max}}}$.

In the present study the reference value of Δh_v, needed for prediction purposes, was measured directly. However, because $K_{c,\text{min}}$ remains constant with geometric similarity of body and cavitated region, it is possible to estimate $(\Delta h_v)_{\text{max=ref}}$ without measuring cavity pressure directly. In a given flow device, two different tests are made in which the free-stream pressure requirements $(h_0 - h_v)$ to obtain geometrically similar cavitated regions are measured. These tests need not be for the same liquid, temperature, velocity, or model scale; however, at least one of these tests must yield measurable thermodynamic effects of cavitation $(\Delta h_v > 0)$. From these measured free-stream pressure requirements, it is possible to determine a $(\Delta h_v)_{\text{ref}}$ value using an iterative process as described in reference 14.

CONCLUDING REMARKS

A method for predicting thermodynamic effects of developed cavitation in venturis, or other flow devices, has been developed. The prediction method, formulated from simple theoretical analyses and supporting experimental cavitation studies, provided good agreement between predicted and experimental results for geometrically scaled venturis handling liquids of widely diverse physical properties. The prediction method accounts for changes in liquid, liquid temperature, flow velocity, cavity length, and model scale, provided that similarity of the cavitating flow is maintained.

The method requires a known reference value of the maximum cavity-pressure depression at one operating condition, obtained either by direct measurement or from two appropriate tests wherein stream static pressure is measured under conditions of similarity of the cavitating flow. These latter test data need not necessarily be for the same liquid, temperature, velocity, or model scale.

Although the present study is limited to venturis, the basic prediction method has been applied successfully to the prediction of cavitation performance for devices such as pumps and inducers (see ref. 14).

LIST OF SYMBOLS

C_p — noncavitating wall-pressure coefficient, $(h_x - h_0)/(V_0^2/2g)$

c_l — specific heat of liquid, Btu/(lb mass)(°R)

D — free-stream diameter (approach section, fig. 2), in.

g — acceleration due to gravity, 32.2 ft/sec²

$h_{c,min}$ — minimum measured pressure in cavitated region, ft of liquid abs

h_v — vapor pressure corresponding to free-stream or bulk liquid temperature, ft of liquid abs

Δh_v — decrease in vapor pressure corresponding to decrease in liquid temperature, ft of liquid

h_x — static pressure at x, ft of liquid abs

h_0 — free-stream static pressure (approach section, fig. 2), ft of liquid abs

J — mechanical equivalent of heat, 778 (ft)(lb force)/Btu

$K_{c,min}$ — developed cavitation parameter based on minimum cavity pressure, $(h_0 - h_{c,min})/(V_0^2/2g)$

K_v — developed cavitation parameter based on free-stream vapor pressure, $(h_0 - h_v)/(V_0^2/2g)$

k — thermal conductivity of saturated liquid, Btu/(ft)(hr)(°R)

L — latent heat of vaporization, Btu/(lb mass)

NPSH — net positive suction head, ft of liquid

T — liquid temperature, °R

ΔT — decrease in local equilibrium temperature due to vaporization, °R

V_0 — free-stream velocity (approach section, fig. 2), ft/sec

ν_l — volume of saturated liquid, cu ft

ν_v — volume of saturated vapor, cu ft

x — axial distance from minimum noncavitating pressure location (also cavity's leading edge) (fig. 2), in.

Δx — length of cavitated region, in.

α — thermal diffusivity, $k/(\rho_l c_l)$, (sq ft)/hr

ρ_l — saturated liquid density, (lb mass)/(cu ft)

ρ_v — saturated vapor density, (lb mass)/(cu ft)

Subscripts

max — maximum

min — minimum

pred — predicted

ref — reference value obtained by experiment

Superscripts

m, n, p exponents (see eq. (4))

REFERENCES

1. SALEMANN, VICTOR, Cavitation and NPSH Requirements of Various Liquids. *J. Basic Eng.*, Vol. 81, No. 2, June 1959, pp. 167–180.
2. SPRAKER, W. A., The Effects of Fluid Properties on Cavitation in Centrifugal Pumps. *J. Eng. Power*, Vol. 87, No. 3, July 1965, pp. 309–318.
3. STEPANOFF, A. J., Cavitation Properties of Liquids. *J. Eng. Power*, Vol. 86, No. 2, April 1964, pp. 195–200.
4. MENG, PHILLIP R., *Change in Inducer Net Positive Suction Head Requirement with Flow Coefficient in Low Temperature Hydrogen (27.9° to 36.6° R).* NASA TN D–4423, 1968.
5. MOORE, ROYCE D., AND PHILLIP R. MENG, *Cavitation Performance of Line-Mounted 80.6° Helical Inducer in Hydrogen.* NASA TM X–1854, 1969.
6. MENG, PHILLIP R., AND ROBERT E. CONNELLY, *Investigations of Effects of Simulated Nuclear Radiation Heating on Inducer Performance in Liquid Hydrogen.* NASA TM X–1359, 1967.
7. RUGGERI, ROBERT S., AND THOMAS F. GELDER, *Cavitation and Effective Liquid Tension of Nitrogen in a Tunnel Venturi.* NASA TN D–2088, 1964.
8. GELDER, THOMAS F., ROBERT S. RUGGERI, AND ROYCE D. MOORE, *Cavitation Similarity Considerations Based on Measured Pressure and Temperature Depressions in Cavitated Regions of Freon–114.* NASA TN D–3509, 1966.
9. MOORE, ROYCE D., AND ROBERT S. RUGGERI, *Venturi Scaling Studies on Thermodynamic Effects of Developed Cavitation of Freon–114.* NASA TN D–4387, 1968.
10. MOORE, ROYCE D., AND ROBERT S. RUGGERI, *Prediction of Thermodynamic Effects of Developed Cavitation Based on Liquid-Hydrogen and Freon–114 Data in Scaled Venturis.* NASA TN D–4899, 1968.
11. HORD, JESSE, DEAN K. EDMONDS, AND DAVID R. MILLHISER, *Thermodynamic Depressions within Cavities and Cavitation Inception in Liquid Hydrogen and Liquid Nitrogen.* Report 9705, National Bureau of Standards (NASA CR–72286), March 1968.
12. STAHL, H. A., AND A. J. STEPANOFF, Thermodynamic Aspects of Cavitation in Centrifugal Pumps. *Trans. ASME*, Vol. 78, No. 8, November 1956, pp. 1691–1693.
13. HOLLANDER, A., Thermodynamic Aspects of Cavitation in Centrifugal Pumps. *ARS J.*, Vol. 32, No. 10, October 1962, pp. 1594–1595.
14. RUGGERI, ROBERT S., AND ROYCE D. MOORE, *Method for Prediction of Pump Cavitation Performance for Various Liquids, Liquid Temperatures, and Rotative Speeds.* NASA TN D–5292, 1969.

DISCUSSION

J. HORD (National Bureau of Standards): The author and his co-workers are to be commended for extending the B-factor[1] theory and synthesizing previous efforts (refs. 1, 2, 12, D–1, D–2) to develop a practical and effective solution to a complex and difficult problem. The "quasi-static" theory upon which the solution is based is amazingly simple, and one cannot help but wonder why it works so well (ref. 14); nevertheless, it must be concluded that the solution, though simplified, contains the significant groups of dimensionless parameters. A current research program (ref. D–3) is endeavoring to upgrade the thermostatic approach outlined in this paper and account for dynamic effects via entrainment theory. Test results from this program indicate that $K_{c,\min}$ for a zero-caliber ogive varies with cavity length as suspected by Ruggeri.

I feel that the author should warn the reader that equation (3) may be a rather crude expression for relating Δh_v and B when the fluid properties vary appreciably with temperature; as evidenced by the nonlinearity of the curves in figure 1b, this is particularly true for liquid hydrogen. Solution of equation (2) in incremental form as outlined by the author in reference 8 is more appropriate for general use. Still a more direct approach for computing B-factor is given below: Hollander (ref. 13) showed that various B-factor solutions (refs. 12, D–1, D–2) were equivalent and could be represented by a "quasi-static" model; this model features a unit mass of liquid confined in an insulated cylinder with a nonleaking piston. When the piston is lifted, we will assume that the fluid undergoes an isentropic expansion. The mass-entropy balance may be written

$$m_1 s_1 = m_{f2} s_{f2} + m_{v2} s_{v2} \tag{D–1}$$

and conservation of mass requires that

$$m_1 = m_{f2} + m_{v2} \tag{D–2}$$

Combining equations (D–1) and (D–2) and multiplying the result by ρ_{f2}/ρ_{v2}, we obtain

$$B = \left(\frac{\rho_{f2}}{\rho_{v2}}\right)\left(\frac{m_{v2}}{m_{f2}}\right) = \left(\frac{\rho_{f2}}{\rho_{v2}}\right)\left(\frac{s_1 - s_{f2}}{s_{v2} - s_1}\right) \tag{D–3}$$

---

[1] $B = V_v/V_l$

where

m_1 = initial mass of liquid

m_{f2} = mass of saturated liquid at final pressure

m_{v2} = mass of saturated vapor at final pressure

s_1 = specific entropy of saturated liquid at initial pressure

s_{f2} = specific entropy of saturated liquid at final pressure

s_{v2} = specific entropy of saturated vapor at final pressure

ρ_{f2} = density of saturated liquid at final pressure

ρ_{v2} = density of saturated vapor at final pressure

This result does not depend on summation of incremental steps to account for changing fluid properties, vaporization of liquid, recondensation of vapor, and so on. The results are as accurate as the fluid P-V-T data; charts, tables, etc., may easily be developed from appropriate equations of state or tabulated thermodynamic properties.

The author emphasizes that local thermodynamic equilibrium within the cavitated region is a prerequisite for application of the B-factor theory. The "quasi-static" model requires only that thermodynamic equilibrium prevail during the vaporization process; consequently, only the *leading edge* of the developed cavity must be in thermodynamic equilibrium. The central and trailing edges of the cavity, where condensation occurs, may not be in stable thermodynamic equilibrium. Recent experiments at NBS with the 0.7-scale venturi substantiate metastability in the central and aft regions of vaporous hydrogen cavities. The experimentally determined exponents in equation (5) are based on pressures measured within the cavity near the leading edge, where equilibrium prevailed in all fluids tested. It appears that the experimental conditions under which the exponents were determined are compatible with the thermostatic theory, and local equilibrium *throughout* the cavitated region is not required. It also appears plausible that exponents derived in this manner could easily account for slight metastabilities (or perhaps unstable equilibria) within vaporous cavities.

I heartily agree with the author that more data are needed to substantiate the exponent for D/D_{ref} in equation (5). For the scale factor studied, the diameter-dependence is less than 4 percent—combining the last two terms in equation (5). For geometrically similar cavities, the last term in equation (5) goes to unity and the diameter-dependence is still less than 8 percent.

M. L. BILLET AND J. W. HOLL (The Pennsylvania State University): The research reported by the author constitutes a valuable contribution to the understanding of thermodynamic effects on developed cavitation. Mr. Ruggeri is to be complimented for his measurement of the effect and its correlation with possible scaling parameters. Also, the corre-

lation of data by means of the B-factor theory is very encouraging. Our comments are primarily restricted to introducing an alternate approach to the B-factor method based on convective heat transfer (ref. D-3).

From the B-factor theory of Stahl and Stepanoff (ref. 12), the temperature depression is given by

$$\Delta T = B \cdot \left(\frac{\rho_v}{\rho_L}\right) \cdot \left(\frac{L}{C_L}\right) \tag{D-4}$$

where B is defined as the ratio of vapor volume to liquid volume and must be determined in terms of scaling parameters of the system. However, the vapor volume is proportional to the product of cavity length and cavity thickness, and also the liquid volume is proportional to the cavity length and thickness of the liquid layer supplying the heat of vaporization. Thus, B must be a function of a maximum cavity diameter divided by the liquid thickness for a body of revolution.

Previous investigators have shown that for water at ordinary temperatures the ratio of maximum cavity diameter to model diameter is solely a function of the cavitation number based on cavity pressure, which in turn is a function of the geometry.

According to the analysis of Gelder, Ruggeri, and Moore (ref. 8), based on the analysis of Eisenberg and Pond (ref. D-4), the liquid thickness is proportional to $\sqrt{\alpha \Delta X / V_0}$. Assuming that the cavities are geometrically similar, the expression for the B-factor for an axisymmetric flow is

$$B = \left(\frac{\Delta X}{D}\right)^{0.5} \cdot \left(\frac{DV_0}{\alpha}\right)^{0.5} C \tag{D-5}$$

where V_0 is the velocity in the uniform stream. It was assumed that C was a universal constant and could be evaluated from a reference state. Denoting the reference state with the subscript "ref," it follows that

$$C = \frac{B_{\text{ref}}}{(V_0 D / \alpha)_{\text{ref}}^{0.5} (\Delta X / D)_{\text{ref}}^{0.5}} \tag{D-6}$$

Employing equation (D-6) in equation (D-5) for C gives

$$B = B_{\text{ref}} \left(\frac{\alpha_{\text{ref}}}{\alpha}\right)^{0.5} \left(\frac{V_0}{V_{0_{\text{ref}}}}\right)^{0.5} \left(\frac{D}{D_{\text{ref}}}\right)^{0.5} \left[\frac{(\Delta X / D)}{(\Delta X / D)_{\text{ref}}}\right]^{0.5} \tag{D-7}$$

Application of equation (D-7) to venturi results indicated that the actual exponents did not agree with theory. Thus, the exponents in equation (D-7) were altered empirically, resulting in equation (5) of the paper.

An alternate approach to correlating data for the thermodynamic effect is the entrainment theory, which is similar to that proposed by Acosta and Parkin (ref. D-5) and later by Plesset (ref. D-6). In this

theory the latent heat requirement is equated to the convective heat transfer at the cavity wall. From this theory, the temperature depression is given by

$$\Delta T = \frac{C_Q}{\mathrm{Nu}} \frac{P_e}{A_w/D^2} \left(\frac{\rho_v}{\rho_L}\right) \left(\frac{L}{C_L}\right) \tag{D-8}$$

where the entrainment coefficient, C_Q, is defined as

$$C_Q = \frac{Q_v}{V_0 D^2} \tag{D-9}$$

and where

  $A_w =$ surface area of the cavity through which the heat transfer occurs
  $Q_v =$ volume flow rate of the vapor in the cavity
  Nu $=$ Nusselt number, $h\Delta X/K$
  $h =$ film coefficient for convective heat transfer
  $P_e =$ Peclet number, $V_\infty \Delta X/\alpha$

In order to apply equation (D-8), it is necessary to determine the three dimensionless parameters C_Q, Nu, and A_w/D^2.

The cavitation number based on cavity pressure, P_c, is defined as

$$K_c = \frac{P_0 - P_c}{\frac{1}{2}\rho_L V_0^2} \tag{D-10}$$

where P_0 is the free-stream pressure. Similarity for developed cavitation in the absence of significant viscous or gravity effects is provided if the cavitation number is constant. This result has been verified by numerous experiments in water at ordinary temperatures. The similarity law was applied to a zero-caliber ogive model (ref. D-3), and the entrainment coefficient, C_Q, was found by creating a similar ventilated cavity and measuring the volume flow rate. The area coefficient, A_w/D^2, was determined from photographs taken of the ventilated cavity. The Nusselt number was assumed to be of the form

$$\mathrm{Nu} = aR_e^b P_r^c F_r^d \tag{D-11}$$

where R_e, P_r, and F_r are the Reynolds, Prandtl, and Froude numbers, respectively. The constants, a, b, c, and d in equation (D-11) were determined by substituting the measured values of ΔT, C_Q, and A_w/D^2 and equation (D-11) into equation (D-8) and then solving for the constants.

The equation for the temperature depression for the *entrainment theory applied to the zero-caliber ogives* was found to be

$$\Delta T = \mathrm{constant}\ g^{0.175} \left[\frac{\rho_v}{\rho_L}\right] \left[\frac{L}{C_L}\right] \left[\frac{1}{\alpha}\right]^{0.55} \left[\frac{1}{\nu_L}\right]^{0.10} \left[\frac{\Delta X}{D}\right]^{0.58} V_0^{0.3} D^{0.825} \tag{D-12}$$

The corresponding equation for the *B-factor theory applied to the venturis* as employed in the paper is

$$\Delta T = \text{constant} \left[\frac{\rho_v}{\rho_L}\right] \left[\frac{L}{C_L}\right] \left[\frac{1}{\alpha}\right] \left[\frac{\Delta X}{D}\right]^{0.3} V_0^{0.8} D^{0.2} \qquad \text{(D-13)}$$

The dimensionless constant in equation (D-12) is equal to 0.495×10^{-3}, whereas the constant in equation (D-13) is dimensional.

A comparison of equations (D-12) and (D-13) indicates that the *B*-factor theory applied to the venturis results in $\Delta T \alpha (\Delta X/D)^{0.3} V_0^{0.8}$, whereas the entrainment theory applied to the ogive yields $\Delta T \alpha (\Delta X/D)^{0.58} V_0^{0.3}$. Thus the effect of velocity is greater for the venturis, but the effect of cavity length to diameter ratio, $\Delta X/D$, is greater for the ogive.

Referring to equations (D-12) and (D-13), it is seen that $\Delta T \alpha D^{0.2}$ for the *B*-factor theory applied to the venturis, whereas $\Delta T \alpha D^{0.825}$ for the entrainment theory applied to the ogive. Thus the implication is that the effect of size is greater for the ogive. However, this has not been verified experimentally, since D was not a variable in the ogive test program; thus D enters as a constant in equation (D-12). Nevertheless, in order for equation (D-12) to be dimensionally correct, it is necessary that the exponent for D be 0.825. It is intended that the size effect will be checked in subsequent investigations of the ogives.

Referring to the fluid property effects in equations (D-12) and (D-13), it is seen that the influence of (ρ_v/ρ_L) and (L/C_L) are the same in both cases, but the exponent on α differs. Also, the entrainment theory contains the additional term $(1/\nu_L)^{0.1}$, which arises from the kinematic viscosity appearing in the Reynolds and Prandtl numbers in the assumed relation for the Nusselt number.

In addition to the above-mentioned differences between the results for the venturis and ogives is the variation of cavitation number with $\Delta X/D$. As indicated in the paper, the cavitation number based on minimum cavity pressure is independent of $\Delta X/D$ for the venturis, whereas for the ogives the cavitation number decreases as $\Delta X/D$ increases (ref. D-3).

Equation (D-12), which was obtained from tests with a zero-caliber ogive in water from 80° to 290° F was employed to predict the behavior of a zero-caliber ogive in Freon-113 from 75° to 190° F. The comparisons between equation (D-12) and the experiment were found to be very good (ref. D-3). As indicated in the paper, equation (D-13) has been applied to venturi data obtained with several liquids, and the correlations have been encouraging.

The aforementioned comparisons between the results for venturis and zero-caliber ogives show that the effects of fluid properties are not in complete agreement and that the major differences appear to be in the

effects due to velocity, size, and relative cavity length. This implies a need to emphasize the investigation of the influence of changes in boundary shape and size on the thermodynamic effect.

F. G. HAMMITT (University of Michigan) : I am interested in whether or not the NASA program has included any measurements of void fraction in the cavity. The appreciable pressure drop measured across the cavity length in the venturi tests seems to indicate the presence of considerable liquid within this cavity. I believe such measurements could be obtained fairly easily by gamma-ray (or X-ray) densitometry, as we once did in our laboratory in a cavitating venturi (ref. D–7). More detailed information on the mechanics of the actual flow could be very useful in improving the realism of the model.

RUGGERI (author) : I wish to thank all the discussors for their timely and very worthwhile comments. First, with regard to Mr. Hord's discussion, I completely agree that equation (3) of the paper does not necessarily provide a good approximation of the vapor-to-liquid-volume ratio curves (*B*-factors), and one should indeed use caution in applying this relation in cases where the physical properties of the liquid and its vapor change significantly with temperature. The method for determining volume ratio, as outlined by Mr. Hord, is more direct and simple and provides ultimate accuracy without the need for solving equations in incremental form to account for changes in fluid properties as the temperature drops due to vaporization. On the question of thermodynamic equilibrium within the cavitated region, it should be pointed out that although the experimentally determined exponents of equation (5) were based on conditions in the cavity's leading-edge region, where equilibrium conditions existed, the final correlations presented in figure 10 included considerable liquid-hydrogen data which exhibited various degrees of metastability in the central and rearward portions of the cavity. No trend was noted in the degree of this metastability. Thus, it appears that conditions of thermodynamic equilibrium need only exist in the leading-edge region to satisfy the present prediction method. This implies that vaporization is confined primarily to the cavity's leading-edge region, with the process for the remainder of the cavity being mostly one of condensation.

Mr. Billet and Dr. Holl are to be commended for their efforts toward the development of a different cavitation model via the entrainment theory. The NASA studies were based on a "quasi-static" conduction model, which admittedly does not properly represent the real flow situation. This may be borne out by the fact that the experimentally determined exponents varied somewhat from the theoretical values based on a pure conduction process. However, it is interesting to note that, with one exception, the parameters for both theories are the same. Nevertheless,

the entrainment theory, which is based on a dynamic—or convective—model, better represents the real flow situation and thus is more sound from a theoretical standpoint. From the standpoint of experimentation, however, the entrainment theory involves certain problems similar to those encountered with the present cavitation model in the determination of absolute rather than effective values of parameters such as C_Q and h. For example, the volume flow rate measured for a ventilated cavity may not necessarily equal the volume flow rate of vapor for a similar vaporous cavity.

The studies of Dr. Holl and his coworkers indicate that for zero-caliber ogives, the value of $K_{c,min}$ changes with cavity length. This is an interesting finding, since, during the venturi studies, it had been suspected that this variance of $K_{c,min}$ with cavity length might occur for different venturis (or body shapes), but it was not verified. Unquestionably, body shape (i.e., noncavitating wall pressure distribution) influences the thermodynamic effects of cavitation in general, and this effect is probably the primary reason for the difference in exponents between the entrainment and modified B-factor theories. The influence of body shape is likely to preclude the prediction of absolute values of thermodynamic effects for arbitrary bodies and liquids for considerable time to come. Much research is needed in this area, but a more immediate need appears to be the influence of body scale on the thermodynamic effects of cavitation.

With regard to Dr. Hammitt's comments, no attempt was made to measure the void fraction in vaporous cavities. Attempts were made to determine whether macroscopic droplets, wall rivulets, etc., were present within the cavity, and, except for isolated instances (particularly for liquid nitrogen), none was found. The axial pressure gradients within vaporous cavities, in my opinion, are due in large part to the velocity (dynamic head) of the vapor, which of course implies very high axial velocities in the extreme leading-edge region and comparatively low velocities in the collapse region. At the time the NASA Lewis program was phased out, plans were to make total and static pressure measurements within vaporous cavities to prove or disprove this concept.

REFERENCES

D-1. Jacobs, R. B., Prediction of Symptoms of Cavitation. *J. Res. Natl. Bur. Std.*, Sec. C., Vol. 65, No. 3, July–September 1961, pp. 147–156.
D-2. Fisher, R. C., Discussion of A Survey of Modern Centrifugal Pump Practice for Oilfield and Oil Refining Services by N. Tetlow. *Proc. Inst. Mech. Engrs.*, Vol. 152, January–December 1945, pp. 305–306.
D-3. Billet, M. L., *Thermodynamic Effects on Developed Cavitation in Water and Freon–113*, M.S. thesis, Aerospace Eng. Dept., Penn. State U., March 1970.

D–4. EISENBERG, P., AND H. POND, *Water Tunnel Investigations of Steady State Cavities*. David Taylor Model Basin Report 668 (Carderock, Md.), October 1948.

D–5. HOLL, J. W., AND G. F. WISLICENUS, Scale Effects on Cavitation. *J. Basic Eng., Trans. ASME*, Series D, Vol. 83, 1961, pp. 385–398. (See discussion by A. Acosta and B. R. Parkin.)

D–6. PLESSET, M. S., *Remarks on Thermal Effects on Cavitation*. Discussion booklet for Symposium on Cavitation State of Knowledge, ASME, 1970.

D–7. SMITH, W., G. L. ATKINSON, AND F. G. HAMMITT, Void Fraction Measurements in a Cavitating Venturi. *Trans. ASME, J. Basic Eng.*, June 1964, pp. 265–274.